

SYNTHESIS AND CHARACTERIZATION OF IRON OXIDE (Fe₃O₄) PARTICLES BY CHEMICAL METHOD AND ITS APPLICATION

Aye Aye Mar¹, Myat Kyaw Thu², Thida³, Ni Ni Than⁴

Abstract

Iron oxide particles with appropriate surface chemistry exhibit many interesting properties that can be exploited in a variety of biomedical application such as magnetic resonance imaging contrast enhancement, tissue repair, hyperthermia, drug delivery and in cell separation. In this study, FeSO₄.7H₂O, NaNO₃ and NaOH were used in the preparation of iron oxide by chemical method. The characteristic properties of iron oxide were studied by X-ray Diffraction (XRD), Fourier Transform Infrared (FT IR) spectroscopy and Scanning Electron Microscopy (SEM) and Thermogravimetric-Differential Thermal Analysis (TG-DTA). The crystalline nature of the prepared iron oxide was identified by XRD analysis. According to XRD data synthesized iron oxide (Fe₃O₄) by chemical method at 100 °C was naturally stabilized cubic structure and in the average crystallite size of 39.27 nm. In FT IR spectrum of iron oxide the peaks at 895 cm⁻¹ and 457cm⁻¹ are due to the vibration of Fe-O group. The SEM micrographs of iron oxide prepared by chemical method at 100°C indicated that the particles are spherical in shape with a narrow size distribution. TG-DTA analysis showed two endothermic peaks and one exothermic peak. Sorption properties of the prepared iron oxide was studied by model congo red dye. Since, the value of separation factor R_L (from Langmuir isotherm) for this dye was 0.04, the adsorption was favourable adsorption.

Keywords: iron oxide, chemical method, congo red, separation factor, Langmuir isotherm

Introduction

Iron and oxygen are two of the four most common elements in the Earth's crust, and iron oxide form naturally through the weathering of Fe-containing rocks both on land and in the oceans. Iron oxides are chemical compounds composed of iron and oxygen. All together there are sixteen known iron oxides and oxyhydroxides. Iron oxides and oxyhydroxides are widespread in nature, play an important role in many geological and biological process, and are widely used by humans, e.g., as iron ores, pigments, catalyst, in thermite and hemoglobin. Common rust is a form of iron (III) oxides (Gareth, 2016). Iron oxide nanoparticles are iron oxide particles with diameters between about 1 and 100 nm. They have attracted much attention due to their fine magnetic properties and applications in modern science. The most common iron oxides for biomedical applications are magnetite (Fe₃O₄) and maghemite (γ-Fe₂O₃). Magnetite is a black magnetic mineral and is also called iron (II, III) oxide or ferrous ferrite. The molecular formula, Fe₃O₄, can also be written as FeO.Fe₂O₃, which consists of wüstite (FeO) and hematite (Fe₂O₃). It has the strongest magnetism of all the natural minerals existing on the earth (Majewski and Thierry, 2007). Magnetite (Fe₃O₄) has an inverse spinel structure with oxygen forming a face-centered cubic system. In magnetite, all tetrahedral sites are occupied by Fe³⁺ and octahedral sites are occupied by both Fe³⁺ and Fe²⁺. Maghemite (γ-Fe₂O₃) differs from magnetite in that all or most of the iron is in the trivalent state (Fe³⁺) and by the presence of cation vacancies in the octahedral sites. Maghemite has a cubic unit cell in which each cell contains 32 O²⁻ ions, 21^{1/3}Fe³⁺ ions and 2^{2/3} vacancies. The cations are distributed randomly over the 8 tetrahedral and 16 octahedral sites (Laurent *et al.*, 2008). Magnetic properties of nanomaterials are powerful manipulation and detection tools which are studied for a long time. Since magnetic fields are not harmful organism, magnetic nanoparticles can be used for biomedical in vivo and, of course, in vivo applications. The

¹ Dr, Lecturer, Department of Chemistry, University of Yangon

² Dr, Professor, Department of Chemistry, University of Yangon

³ Dr, Associate Professor, Department of Chemistry, University of Yangon

⁴ Dr, Professor and Head, Department of Chemistry, University of Yangon

latest researchers tell about high potential of magnetic nanoparticles in environments applications such as removal of heavy metals from waste water. Magnetic properties depend on size, shape, structure, crystallinity, synthesis method and chemistry of materials. The most widely investigated magnetic nanomaterials are iron, cobalt and nickel compounds and alloys (Shahoo *et al.*, 2010). Iron (II, III) oxide, chemical formula Fe_3O_4 or Fe_2O_3 . Black or grayish black colour mineral. Structure formula $[\text{Fe}^{3+}]_T \text{d}[\text{Fe}^{3+}\text{Fe}^{2+}]_O \text{Oh O}^{2-}$, which means there is tetrahedral magnetic sub lattice, containing Fe^{3+} ions, an octahedral sub lattice, containing Fe^{3+} and Fe^{2+} ions. Spins from these two sub lattices are antiparallel so magnetite and magnetization occurs due to Fe^{2+} ions from octahedral sub lattice. Magnetite is sensitive to oxidation-oxygen transforms it to maghemite by oxidizing of Fe^{2+} ions (Lodhia *et al.*, 2010)

Materials and Methods

Preparation of Iron Oxide

A 14 g of NaOH (0.35 mol) and 4.2495g of NaNO_3 (0.05 mol) were placed into a 1L beaker containing 150 mL distilled water. Then the volume was made up to 300 mL with distilled water. A 36.84 g of $\text{FeSO}_4 \cdot 7\text{H}_2\text{O}$ was dissolved in distilled water and the volume made up to 250 mL in a 250 mL volumetric flask. The FeSO_4 solution was slowly added into the beaker containing solution mixture of NaOH and NaNO_3 . The black precipitate was obtained and the sample was aged at room temperature for 16 days. Then, the sample was washed and filtered and then dried at temperature of 100 °C.

Characterization of the Prepared Iron Oxide Samples

Prepared iron oxide particles were qualitatively analyzed by X-ray diffractometer. Infrared Spectrometer (FT IR) with a scan speed of 16 scans/sec from 400 to 4000 cm^{-1} was used to identify the functional groups present in the sample. The SEM micrograph was obtained using JXA 840 A, JEOL Ltd., Japan, the permanent records obtained by the crystals feature. Thermal stability of the prepared sample was evaluated by simultaneous TG-DTA operated under air atmosphere. The measurements were carried out at a heating rate of 10.0 °C min^{-1} and scanning from 30 °C to 600 °C.

Determination of Wavelength of Maximum Absorption (λ_{max}) of Congo Red and Construction of the Calibration Curve

To determine the wavelength of maximum absorption (λ_{max}) of congo red solution the absorbance values were recorded in the visible range of 400 - 600 nm by using using a UV-visible spectrophotometer. The calibration curve of congo red solution was constructed by using different concentrations of 10, 20, 30, 40 and 50 ppm solutions at the wavelength of maximum absorption of congo red.

Sorption of Congo Red on the Prepared Iron Oxide sample

Study on the effect of contact time on removal of congo red dye

A 0.5 g of magnetite was placed into the separate conical flasks and treated with 50 mL 30 ppm congo red solution at pH of 7. These experiments were performed with the same concentration of dye solution and the same amount of iron oxides samples. The flasks containing congo red and iron oxides as adsorbents were placed in the thermostatic shaker at room temperature. The contact time settings were 20,40,60,80,100 and 120 min. After shaking, the sample solutions were filtered off and the filtrates were spectrophotometrically measured at λ_{max}

495 nm. By the contact time setting, the removal percent of congo red dye onto iron oxide was calculated.

Study on the effect of dosage on removal of congo red dye

Dyes removal efficiency of iron oxide was determined by using different weights of 0.2, 0.4, 0.6, 0.8 and 1g. Each 50 mL of 30 ppm congo red solution adjusted to pH 7 was added into separate conical flasks. Then 0.2, 0.4, 0.6, 0.8 and 1g of each sample was added into each conical flask and the solution was agitated in thermostatic shaker at room temperature for 1h. Then the solution was removed from samples by filtration. The absorbance values of resultant solutions were measured at λ_{\max} 495 nm using the spectrophotometer (Jain and Sikarwar, 2006).

Results and Discussion

Iron Oxide Prepared by Chemical Method

In this study, iron oxide was prepared by using chemical method at 100°C. The prepared iron oxides sample was black in colour as shown in Figure 1.



Figure 1 Prepared iron oxide

Characterization of Prepared Iron Oxide Samples

XRD

Figure 2 shows X-ray diffractogram of iron oxide sample obtained at 100 °C. Characteristic peaks of iron oxide appeared at 30.075°, 35.500°, 43.110° 57.049° and 62.662° of 2 θ values with corresponding Miller indices of (220), (311), (400), (511), (440), respectively. The XRD pattern of the prepared iron oxide sample clearly matched with the standard library data of JCPDS-87-2334 magnetite. The diffraction angle, interplanar spacing and Miller Indices of prepared iron oxide sample are shown in Table 1. It was observed that the sample showed single phase of Fe₃O₄ with no impurity phase. The resultant iron oxide was indexed as cubic structure with a= 8.3851 Å (Table 2). Average crystallite size of prepared iron oxide sample was calculated by using Scherrer equation,

$$t = \frac{K\lambda}{\beta \cos\theta}$$

Where t = crystallite size in nanometers
 K = Scherrer constant
 θ = Diffraction angle of the peak under consideration of FWHM (°)
 λ = wavelength (Å)
 β = the broadening solely due to small crystallite size (FWHM radians).

The average crystallite size was found to be 39.27 nm.

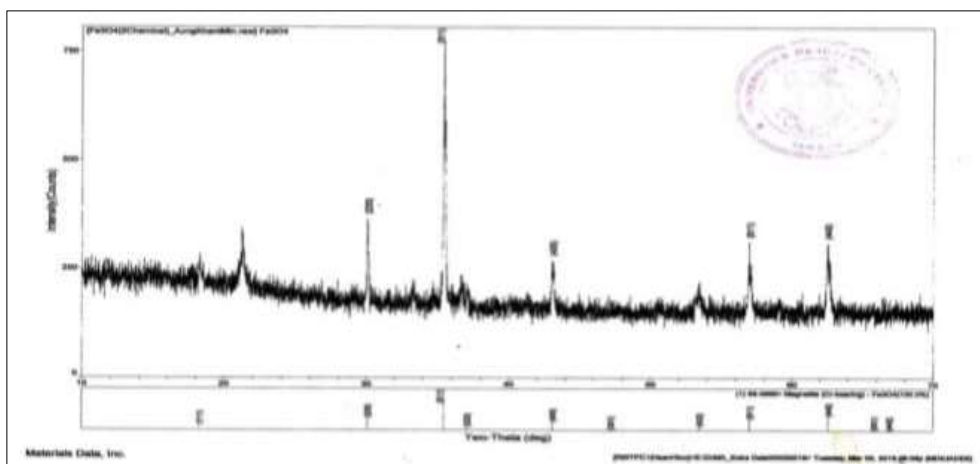


Figure 2 X-ray diffractogram of prepared iron oxide

Table 1 Diffraction Angle, Interplanar Spacing and Miller Indices of Prepared Iron Oxide

No.	Diffraction angle (2θ) (degree)	Interplanar spacing (Å)	Miller indices			Remark
			h	k	l	
1.	18.291	4.8463	1	1	1	Fe ₃ O ₄
2.	30.075	2.9689	2	2	0	Fe ₃ O ₄
3.	35.500	2.5266	3	1	1	Fe ₃ O ₄
4.	37.124	2.4198	2	2	2	Fe ₃ O ₄
5.	43.110	2.0966	4	0	0	Fe ₃ O ₄
6.	47.179	1.9248	3	3	1	Fe ₃ O ₄
7.	53.450	1.7128	4	2	2	Fe ₃ O ₄
8.	57.049	1.6130	5	1	1	Fe ₃ O ₄
9.	62.662	1.4814	4	4	0	Fe ₃ O ₄
10.	65.755	1.4190	5	3	1	Fe ₃ O ₄
11.	66.913	1.3972	4	4	2	Fe ₃ O ₄

Table 2 Crystal Structure, Lattice Constant and Average Crystallite Size of Prepared Iron Oxide

No.	Sample	Crystal structure	Lattice constant (Å)	Average crystallite size (nm)
1.	Iron oxide	Cubic	8.3851	39.27

FT IR

Figure 3 shows FT IR spectrum of iron oxide sample obtained at 100 ° C and the spectral data are shown in Table 3. The absorption band at 3451 cm⁻¹ was due to stretching vibration of hydroxyl functional group (O-H) on the surface of oxide particles or adsorbed water in the sample. Absorption peaks at 895 cm⁻¹ and 457 cm⁻¹ are due to the vibration of Fe-O group in prepared iron oxide particles.

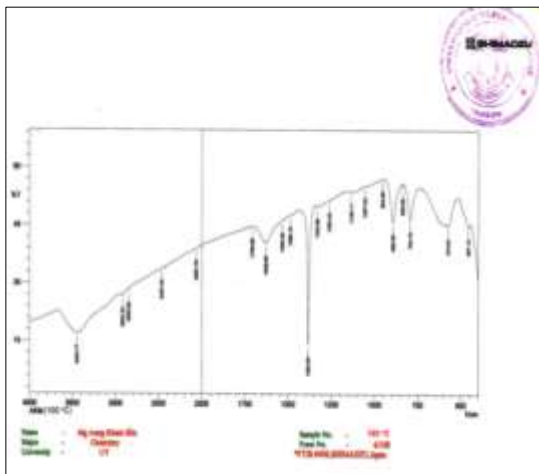


Figure 3 FT IR spectrum of prepared iron oxide

Table 3 FT IR Spectral Data of Prepared Iron Oxide (Fe₃O₄)

No.	Wavenumber (cm ⁻¹)	Literature value*(cm ⁻¹)	Assignment
1.	3451	3570-3200 (broad)	Stretching vibration of hydroxyl group
2.	895	1010-850(M=O)	Vibration of Fe-O group
3.	457	400-600 (M-O)	Vibration of Fe-O group

*Coates, 2000

Surface morphology of the iron oxide

Surface morphology of the prepared iron oxide sample was studied by using SEM as shown in Figure 4. The image of SEM represents spherical morphology of iron oxide particles. Mostly particles were in sphere form but particles with cubic shape were also observed. The SEM also revealed the agglomeration of iron oxide particles with a narrow size distribution. The particles have a narrow size distribution and the SEM micrograph indicates the porous nature of the surface.

TG- DTA data of iron oxide

TG and DTA curve of prepared iron oxide is shown in Figure 5. The temperature range was 30°C to 600°C. In TG analysis, the total weight loss percentage of the sample was 6.472 %. The initial weight loss observed below 200 °C corresponds to the removal of water existing on the surface of iron oxide. From DTA data, above 200 °C, exothermic peaks and endothermic peaks were observed due to the phase transformation. (Table 4).

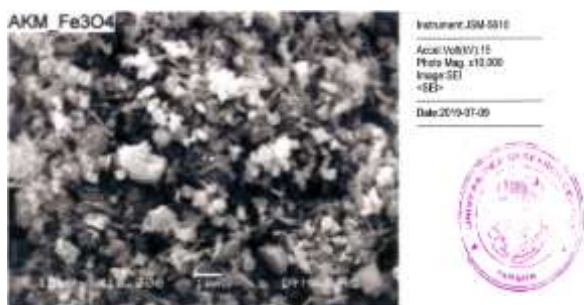


Figure 4 SEM microphotograph of prepared iron oxide

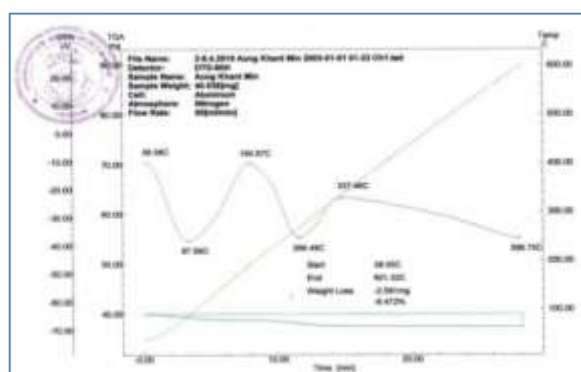


Figure 5 TG-DTA thermogram of prepared iron oxide

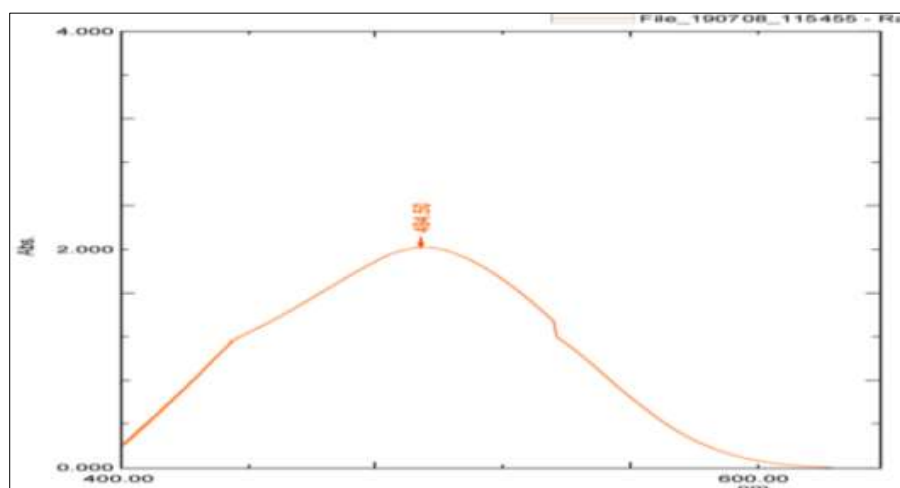
Table 4 TG-DTA Data of Prepared Iron Oxide

No.	Observed Temperature (°C)	Weight Loss (%)	Interpretation
1.	87.89	0.859	Endothermic peak, removal of water existing on the surface
2.	190.87	1.845	Exothermic peak, oxidation reaction takes places
3.	266.49	1.963	endothermic peak, phase transition from Fe ₃ O ₄ to Fe ₂ O ₃ *
4.	337.46	1.805	exothermic peaks, phase transition from Fe ₃ O ₄ to Fe ₂ O ₃ *

*Khan *et al.*,2015

Absorption Spectrum and Calibration Curve of Congo Red

In this research, congo red solution was used to study the effect of sorption by prepared iron oxide. Figure 6 shows the absorption spectrum of congo red solution. The wavelength of maximum absorption was found at 495 nm. Standard calibration curve was constructed using concentrations of standard congo red solution at 495 nm. According to calibration curve (Table 5 and Figure 7), the straight line passed through the origin ($R^2 = 0.9889$) indicating that it obeyed Beer's Law.

**Figure 6** Absorption spectrum of congo red solution**Table 5** Relationship between Absorbance and Concentration of Standard Congo Red Solution

Concentrations (ppm)	Absorbance at 495 nm
10	0.15
20	0.33
30	0.45
40	0.57
50	0.68

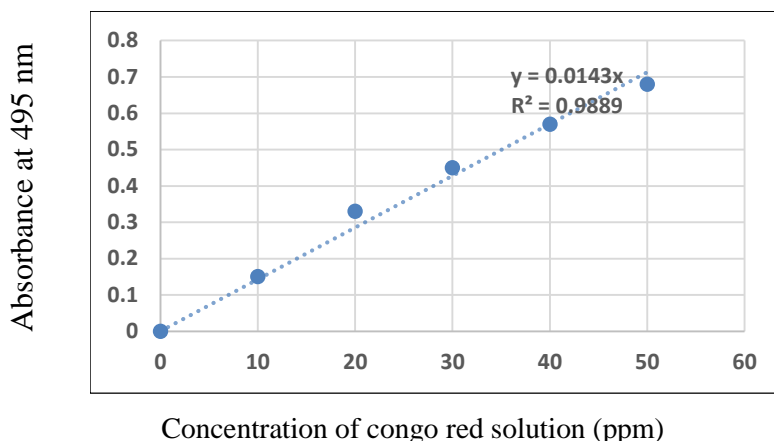


Figure 7 Calibration curve for standard congo red at 495 nm

Sorption of Congo Red onto Prepared Iron Oxide (Magnetite)

Effect of contact time

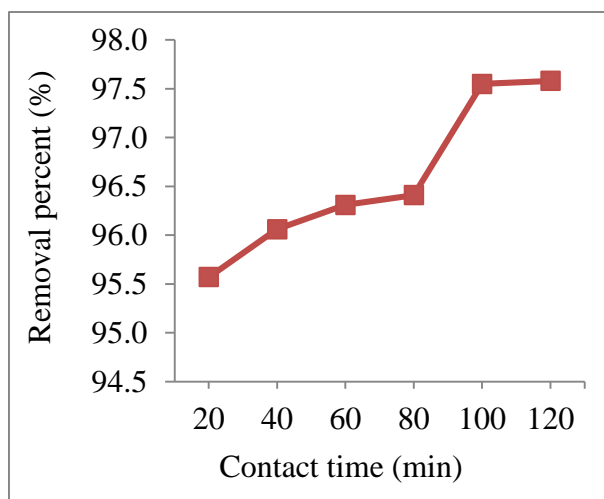
In the present work, sorption capacity of magnetite samples onto congo red was studied. Figure 8 shows a plot of removal percent of congo red as a function of contact time. As the contact time increased removal percent also increased. For the contact time of 120 min, 97.60 % of congo red were removed and adsorbed on magnetite sample.

Effect of dosage

The effect of dosage of the prepared iron oxide samples on the removal of congo red dye was studied by choosing the dosage of the prepared iron oxide samples from 0.2 to 1.0 g. Table 6 shows the relationship between dosage of magnetite with removal percentage of congo red and the corresponding histogram is depicted in Figure 9. By using 1.0 g of magnetite sample and 97.33% of congo red were removed and adsorbed on magnetite sample.

Langmuir Adsorption Parameters

An adsorption isotherm is characterized by certain constants, which express the surface properties and affinity of the adsorbent and can also be used to compare the adsorption capacities of the adsorbent for different adsorbate (Hall *et al.*, 1966). In this study, data from Langmuir plots of congo red sorption onto magnetite sample were obtained (Table 7). The correlation coefficient R^2 for congo red was 0.4751. This value indicated weak binding of congo red dyes to the surface of the magnetite iron oxide sample. The separation factor R_L for congo red was 0.04 (Table 8). R_L is the essential characteristic of the Langmuir isotherm which indicates the shape of isotherm that predicts whether an adsorption is favourable or unfavourable. Since the value of R_L between 0 and 1, sorption of congo red can be considered as favourable adsorption (McKay *et al.*, 1982).



Experimental condition

Amount of magnetite = 0.5 g

Volume of solution = 50 mL

Concentration of dye = 30 ppm

pH = 7

Figure 8 Plot of congo red removal percent as a function of contact time

Table 6 Relationship between Dosage of Magnetite and Percent Removal of Congo Red

Dosage (g)	Absorbance	Ce (mg L ⁻¹)	Ci - Ce (mg L ⁻¹)	Removal (%)
0.2	0.013	0.95	29.05	96.83
0.4	0.014	1.02	28.98	96.60
0.6	0.007	0.51	29.49	98.30
0.8	0.010	0.73	29.27	97.57
1.0	0.011	0.80	29.20	97.33

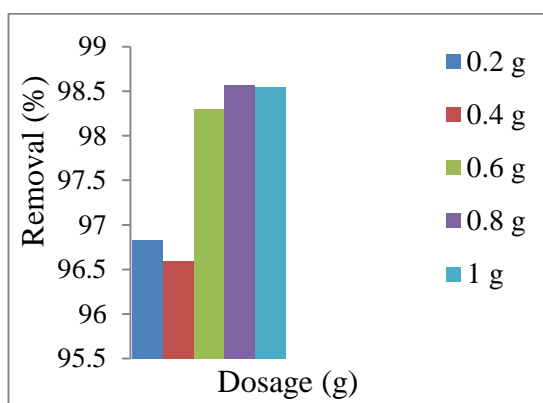


Figure 9 Histogram of removal percent of congo red with dosage of the prepared magnetite sample

Experimental condition

percent pH = 7

Contact time = 1 h

Concentration of dye = 30 ppm

Volume of congo red solution = 50 mL

Table 7 Equilibrium Data for Adsorption of Congo Red by Magnetite

Weight of sample m (g)	Absorbance	Final conc: C _e (mg L ⁻¹)	Amount of absorbed, x (mg)	q _e = x/m (mg g ⁻¹)	1/C _e (L/mg)	1/q _e (gmg ⁻¹)
0.2	0.013	0.95	0.87	4.35	1.05	0.23
0.4	0.014	1.02	0.87	2.18	0.98	0.46
0.6	0.007	0.51	0.88	1.47	1.96	0.68
0.8	0.010	0.73	0.88	1.10	1.37	0.91
1.0	0.011	0.80	0.88	0.88	1.25	1.14

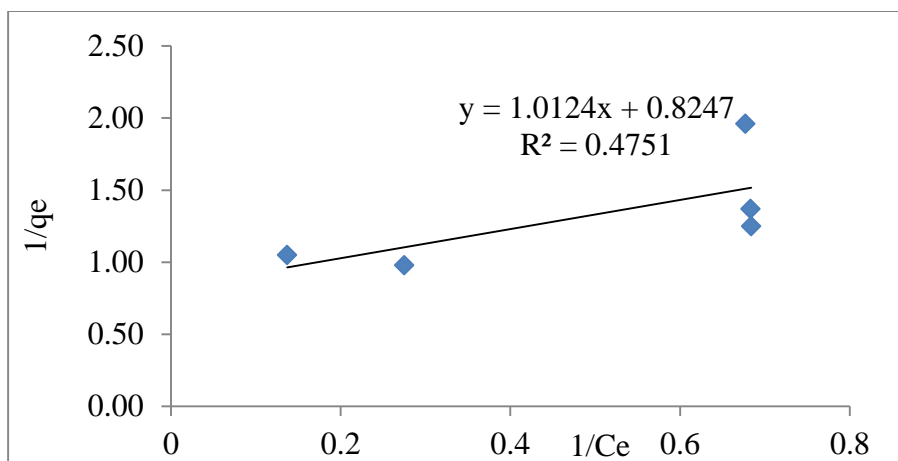


Figure 10 Langmuir plot of congo red adsorption onto magnetite sample

Table 8 Langmuir Isotherm Parameters for the Dyes

Dyes	Sorption coefficient $K_L(x 10^{-2}L mg^{-1})$	Sorption capacity $q_{max} (mg g^{-1})$	Correlation coefficient R^2	Separation factor R_L
Congo red	0.81	1.21	0.4751	0.04

Conclusion

In this study, synthesis of iron oxide (Fe_3O_4) by chemical method was carried out and the dye removal properties of the prepared iron oxide was investigated. XRD data revealed the single phase of Fe_3O_4 with crystallites size of 39.27 nm. The FT IR spectrum of the prepared iron oxide showed the peaks at $895 cm^{-1}$ and $457 cm^{-1}$ corresponding to the vibration of Fe-O groups. The particles are spherical in shape with a narrow size distribution as indicated by SEM. Moreover, iron oxide prepared was studied by TG-DTA analysis, it was found that total weight loss 6.472 %. Two exothermic peaks and two endothermic peaks were corresponding to the vaporization of moisture, phase transition and oxidation reaction takes place in the sample. For the contact time of 120 min, 97.60 % of congo red were sorbed on prepared iron oxide particles. So the prepared iron oxide sample was effective in removal of dyes in waste water treatment. In the dosage of 1g of prepared iron oxide sample in 50 mL of 30 ppm dye solution, percentage of sorbed congo red was 97.33 %. According to Langmuir adsorption parameters, it was found that weak binding of congo red dyes onto the surface of the iron oxide sample since the R^2 value for was 0.4751. Since the value of separation factor R_L for congo red dye was 0.04, the adsorption was favourable adsorption.

Acknowledgements

The authors would like to thank the Department of Higher Education, Ministry of Education, Yangon, Myanmar, for allowing us to carry out this research programme. Thanks are also extended to the Myanmar Academy of Arts and Science and for allowing to present this paper.

References

- Coates, J. (2000). *Interpretation of Infrared Spectra, A Practical Approach*. In Encyclopedia of Analytical Chemistry. Meyers, A., (Ed.), Chichester: 2nd ed. John Wiley and Sons Ltd, p. 10815-10837
- Gareth, S. P. (2016). "Iron Oxide Surfaces". *Surface science*, vol. 71, pp. 272-365
- Hall, K. R., Eagleton, L. C. , Acrivos, A. and Vermeulen, T. (1966). "Pore and Solid Diffusion Kinetics in Fixed-bed Adsorption under Constant-pattern Conditions". *Ing. Eng. Chem. Fund*, vol. 5, pp. 212-223
- Jain, R. and Sikarwar, S. (2006). "Photocatalytic and Absorption Studies on the Removal of Dye Congo red from Wastewater". *Int. J. Environment and Pollution*, vol. 27, pp. 158-160
- Khan, U.S., Amanullah, Manan, A., Khan, N. Mahmood, A. and Rahim, A. (2015). "Transformation Mechanism of Magnetite Nanoparticles". *Materials Science-Poland*, vol. 33(2), pp. 278-285
- Laurent, S., Vander, E.L.M. and Robert, N. (2008). "Magnetic Iron Oxide Nanoparticles: Synthesis, Stabilization, Vectorization, Physicochemical Characterizations and Biological Applications". *Chemical Reviews*, vol. 108, pp. 2064-2110
- Lodhia, J., Mandarano, G., Ferris, N.J., Eu, P. and Cowell, S.F. (2010). "Development and Use of Iron Oxide Nanoparticles (Part I): Synthesis of Iron Oxide Nanoparticles for MRI". *Biomedical Imaging and Intervention Journal*, vol. 6, pp. 1-11
- Majewski, P. and Thierry, B. (2007). "Functionalized Magnetite Nanoparticles-synthesis, Properties, and Bio-applications". *Critical Reviews in Solid State and Material Science*, vol. 32, pp. 203-215
- Mckay, G., Blair, H. S. and Gardner, J. R. (1982). "Adsorption of Dye on Chitin, I. Equilibrium Studies". *J. Appl. Polym. Sci.*, vol. 27, pp. 3043-3057
- Shahoo, S. K., Agrawal, K., Polke, B.G. and Raha, K.C. (2010). "Characterization of γ and α -Fe₂O₃ Nanopowder Synthesized by Emulsion Precipitation Calcination Route and Rheological Behaviour of α -Fe₂O₃", *Inter. J. Engin. Sci & Tech.*, vol.2, pp. 118-126